Am J Cancer Res 2026;16(8):3408-3421
www.ajcr.us /ISSN:2156-6976/ajcr0171308

Original Article

Association between DPAGT1 and Siglec-15 expression and the malignant phenotype of hepatocellular carcinoma

Min Luo[1], Xiaochen Wang[1], Hongzhi Wang[1], Yanping Liu[1], Chaoyuan Huang[1], Haotang Wei[2]

[1]Department of Oncology, The Second Nanning People's Hospital, Nanning 530021, Guangxi, China; [2]Department of Gastrointestinal Surgery, The Second Nanning People's Hospital, Nanning 530021, Guangxi, China

Received January 7, 2026; Accepted August 2, 2026; Epub August 15, 2026; Published August 30, 2026

Abstract: N-acetylglucosamine phosphotransferase 1 (DPAGT1), a key enzyme involved in protein glycosylation, has been implicated in tumor progression; however, its relationship with sialic acid-binding immunoglobulin-like lectin-15 (Siglec-15) in hepatocellular carcinoma (HCC) remains unclear. This study investigated the association between DPAGT1 expression, Siglec-15 expression, and malignant phenotypes in HCC. Bioinformatic analysis of the GEPIA database revealed higher expression of DPAGT1 and Siglec-15 in HCC tissues. Higher DPAGT1 expression was associated with poorer overall survival, whereas Siglec-15 expression showed no significant association with survival outcomes. Although DPAGT1 and Siglec-15 expression levels showed a statistically significant correlation, the correlation strength was weak. Functional experiments demonstrated that DPAGT1 overexpression promoted proliferation, migration, and invasion of HCC cells, whereas DPAGT1 knockdown resulted in reduced malignant phenotypes. Re-expression of Siglec-15 partially alleviated the inhibitory effects associated with DPAGT1 depletion. Similar alterations were observed in Hep-3B cells and a xenograft model, where DPAGT1 modulation was associated with changes in tumor growth, Siglec-15 expression, TGF-β1 levels, AKT phosphorylation, and EMT-related molecular markers. Collectively, these findings suggest that DPAGT1 may contribute to HCC progression and is functionally associated with Siglec-15 expression and EMT-related molecular alterations. Further studies are required to clarify the underlying molecular relationship between DPAGT1 and Siglec-15.

Keywords: Hepatocellular carcinoma, DPAGT1, Siglec-15, correlation, epithelial-mesenchymal transition

Introduction

Hepatocellular carcinoma (HCC) is the sixth most commonly diagnosed cancer worldwide [1]. In China alone, approximately 300,000 individuals die of HCC. Although recent advances in diagnostic technologies have improved early detection of HCC, the high cost of these procedures limits patients' access to early diagnosis [2]. The insidious onset and highly invasive nature of HCC contribute substantially to its rapid progression. Approximately 70% of patients with HCC are diagnosed at advanced stages, missing the optimal window for treatment [3]. Therefore, identifying reliable biomarkers for early clinical diagnosis of HCC is urgently needed. The mechanisms underlying HCC initiation and progression remain poorly understood, but accumulating evidence suggests that genetic alterations accumulate progressively, as observed in many solid tumors. Hepatocarcinogenesis is driven by the accumulation of genetic alterations affecting oncogenes and tumor suppressor genes [4]. N-acetylglucosaminephosphotransferase 1 (DPAGT1) is a key enzyme involved in the initial steps of protein N-glycosylation in the endoplasmic reticulum. Research indicates that elevated DPAGT1 expression is associated with increased cell proliferation and defective maturation of cell-cell adhesion structures [5]. Downregulation of DPAGT1 promotes the maturation of cell-cell adhesion structures and suppresses cell proliferation. Sialic acid-binding immunoglobulin-like lectin 15 (Siglec-15), a member of the Siglec family, contains two immunoglobulin-like domains and is primarily expressed on immune cells. Recognition of sialylated glycans

https://doi.org/10.62347/UYRE7518

plays an important role in immune regulation, making Siglec-15 a promising target for next-generation immuno-oncology therapies [6]. Notably, elevated Siglec-15 expression has been reported in various solid tumors, including lung cancer, breast cancer, head and neck squamous cell carcinoma, and bladder cancer [7].

The DPAGT1 gene encodes a rate-limiting enzyme that plays an important role in regulating the glycosylation of a wide range of proteins [8]. Glycosylation is the most common post-translational modification of proteins. Glycosylation is a critical cellular process that regulates various physiological and pathological activities [9]. Glycosylation also contributes to the regulation of antitumor immune responses and tumor metastasis [10]. Recent studies have revealed that DPAGT1 regulates Siglec-15 expression [11]. Dysregulation of DPAGT1 may result in aberrant N-glycosylation of Siglec-15, thereby affecting its binding affinity for ligands and its capacity to regulate immune cell functions. Previous studies demonstrated that DPAGT1 expression was increased approximately 1.9-fold in HCC tissues compared with normal liver tissues, suggesting that DPAGT1 may contribute to glycosylation dysregulation in HCC [12]. Previous studies have shown that DPAGT1 knockdown inhibits tumor growth, including in HCC models [13]. However, the regulatory relationship between DPAGT1 and Siglec-15 expression in HCC, as well as its clinical significance, remains unclear. This study aimed to analyze the correlation between DPAGT1 and Siglec-15 expression in HCC tissues and investigate their effects on the biological behavior of HCC cells. These findings may provide new insights into the identification of molecular markers for HCC.

Materials and methods

Expression of DPAGT1 and its correlation with Siglec-15 prognosis

The GEPIA database (http://gepia.cancer-pku.cn/) was used to retrieve expression and survival data for DPAGT1 and Siglec-15 in HCC. Differential gene expression was analysed between tumour tissues (n = 369) and adjacent normal tissues (n = 160), using a filtering threshold of $|\log_2$ fold-change$|$ >1 and q-value <0.01. For the survival analysis, the patients were divided into high- and low-expression groups based on the median expression value (default cutoff values for GEPIA and Siglec-15). Kaplan-Meier survival curves were constructed for overall survival (OS).

In vitro cell cultivation

HepG2 cells (Cell Bank of the Chinese Academy of Sciences, Shanghai) and Hep-3B cells (ATCC, Manassas, VA, USA) were authenticated by STR profiling. To ensure experimental consistency, both cell lines were cultured in RPMI-1640 medium (Gibco, USA; Cat. No. 61870036) containing 10% FBS (Gibco, USA; Cat. No. 8121274) and 1% penicillin-streptomycin (Gibco, USA; Cat. No. 15140-148) at 37°C with 5% CO_2. To investigate the biological functions of DPAGT1 and Siglec-15, a series of genetic constructs were generated. These included vectors to overexpress DPAGT1 and Siglec-15 (OE-DPAGT1 and OE-Siglec-15), vectors to interfere with DPAGT1 and Siglec-15 (sh-DPAGT1 and sh-Siglec-15), and siRNAs to target Siglec-15 (si-Siglec-15) and its negative control (si-NC). All plasmids were from GenePharma (Shanghai, China) and transfected into cells using Lipofectamine 2000 (Invitrogen, Carlsbad, USA; Cat. No. 11668019). Overexpression vectors for Siglec-15 and DPAGT1 were generated in the pcDNA3.1 backbone (GenePharma), with an empty pcDNA3.1 vector serving as the negative control.

Mouse xenograft model

Twenty male BALB/c nude mice (4 weeks old, 18-20 g) were obtained from the Experimental Animal Center of the Chinese Academy of Sciences. Hep-3B cells were harvested at 80-90% confluence, resuspended to 2×10^6 cells/mL in PBS, and 100 μL was subcutaneously inoculated into the posterior axillary and inguinal regions of each mouse. When tumors reached 50-100 mm^3, mice were randomly divided into 4 groups (n = 5 per group): OE-vector, OE-DPAGT1, sh-scramble, and sh-DPAGT1. Plasmid or shRNA constructs were complexed with in vivo-jetPEI (Polyplus-transfection, France) at an N/P ratio of 6 according to the manufacturer's instructions to form stable DNA-polymer complexes. A total dose of 100 μg plasmid DNA per mouse was administered via intraperitoneal injection in a final volume of 500 μL every 3 days for a total of three

doses. Tumor volume and body weight were recorded every 7 days. On day 21, mice were euthanized by cervical dislocation under isoflurane anesthesia, and xenografts were excised for measurement and analysis. The modulation of DPAGT1 expression in tumor tissues was confirmed by Western blot analysis. Animal experimental protocols were approved by the Institutional Animal Care and Use Committee of the Second Nanning People's Hospital (Approval No. 20240501).

CCK-8 cell growth assay

Cell growth was assessed with the CCK-8 kit (Solarbio, China; Cat. No. CA1210). Cells were trypsinized, resuspended in complete RPMI-1640 medium, and seeded into a 96-well plate at 2,000 cells/well (100 µL/well). After overnight attachment, cells were treated as indicated, and at 0, 12, 24, and 36 h, 10 µL CCK-8 was added to each well and incubated for 1 h at 37°C, 5% CO_2. Absorbance at 450 nm was measured using a FilterMax F3 microplate reader (MD, USA).

Colony formation assay

Digest cells with 0.25% Trypsin-EDTA (GIBCO, USA; Cat. No. 25200072) to get a single-cell suspension. Resuspend it in PBS and RPMI-1640 medium, count and adjust to 1×10^3 cells/mL. Cells were serially diluted and seeded at defined densities in pre-warmed 6-cm dishes. Incubate at 37°C in a 5% CO_2 atmosphere. After colony formation, wash with PBS, fix with 4% paraformaldehyde (Solarbio, China; Cat. No. BL539A), and stain with 0.1% crystal violet (Solarbio, China; Cat. No. G1063). Colony formation rates were calculated for quantitative evaluation.

RT-qPCR

Total RNA was isolated using TriQuick Reagent (Solarbio, China; Cat. No. R1100) following the manufacturer's recommended protocol. The RNA was reversed into cDNA using the Reverse Transcription Kit (Toyobo, Osaka, Japan; Cat. No. FSQ-101). qPCR was performed on an Agilent AriaMx system using the 2× Universal SYBR qPCR Mix in a 15 µL reaction system (7.5 µL SYBR Mix, 0.6 µL each primer, 1 µL cDNA, 0.3 µL ROX, and 5.0 µL ddH_2O). Thermal cycling consisted of 95°C for 30 s, followed by 40 cycles of 95°C for 5 s and 60°C for 30 s. The relative gene expression levels of DPAGT1, Siglec-15, C-myc, and Cyclin D1 were calculated using the 2-ΔΔCt method. The specific sequences of RT-qPCR primers are detailed in Table S1.

Scratch test

A confluent monolayer was formed by the cells which had been plated in a 6-well plate and left to grow. Twenty-four hours after transfection, cells were pretreated with mitomycin C (1 µg/mL, Solarbio, China; Cat. No. M1181) for 1 h at 37°C, then washed three times with PBS to remove residual drug. A sterile micropipette tip (10 µL) was used to create a vertical scratch in the cell monolayer. Subsequently, the cells were washed three times with PBS and then incubated in serum-free medium in a CO_2 incubator. Morphological changes in each group were observed at 0, 24 and 48 hours using an inverted microscope.

Transwell invasion assay

Cells were pretreated with mitomycin C (1 µg/mL) for 1 h prior to harvest, then seeded into the upper chamber of a Matrigel-coated Transwell insert (Corning, USA; Cat. No. BL539A) at a density of 1×10^5 cells per well, and 1500 µL of RPMI-1640 medium + 10% FBS was added to the lower chamber to establish a chemotactic gradient. The plates were incubated at 37°C for 24 h. After incubation, invaded cells on the lower membrane surface were fixed, stained, and imaged using a Nikon Ts2-FL microscope. Cell counts were obtained from five randomly selected fields per insert using ImageJ.

Co-Immunoprecipitation, Co-IP

Co-IP was performed according to the kit instructions (Thermo, USA; Cat. No. 88828). Cells lysates (RIPA buffer, Solarbio, China; Cat. No. R0010; 30 min on ice) were cleared (12 000×g, 10 min), and 5% of the lysate was reserved as input control. Equal amounts of protein were incubated overnight at 4°C with anti-DPAGT1 antibody (Abcam, ab99518) or control Rabbit IgG plus Protein A/G beads (2 h). Beads were washed, eluted in SDS buffer, boiled 5 min, and analysed by Western blot for Siglec-15 and DPAGT1 to detect endogenous protein expression.

Immuno-fluorescence antibody test

Plate cells on coverslips in 6-well plates. When cell confluency reaches ~30%, wash with PBS. Fix cells with fixative for 15 min, then wash thrice with PBS. Permeabilize cells with 0.1% Triton X-100 for 10 min and wash thrice with PBS. Block with immunostaining blocking solution for 15 min. Incubate coverslips with rabbit monoclonal antibody against Siglec-15 (1:200) for 1 h, followed by Alexa Fluor 488-conjugated goat anti-rabbit IgG (1:200) for 1 h. Then DAPI 5 min and rinse. Add anti-fluorescence quenching sealing solution and cover with cover glasses. Capture images using a Nikon Ts2-FL fluorescence microscope at 200× magnification under identical exposure settings. The mean fluorescence intensity was quantified using ImageJ software by randomly selecting five fields per sample.

Western blot analysis (WB)

Total protein was extracted from cells or nude mouse tumors using RIPA-PMSF buffer (Solarbio, China; Cat. No. R0010), and the concentration was determined with a BCA kit (Solarbio, China; Cat. No. PC0020). Samples were separated on 10% SDS-PAGE (90 V for 20 min, then 120 V for 60 min) and transferred to a PVDF membrane (Millipore, USA; Cat. No. IPVH00010) by wet transfer at 300 mA for 70 min. Membranes were blocked for 1 h at room temperature in 5% skimmed milk, incubated with primary antibodies overnight at 4°C, washed with TBST, and then incubated with HRP-conjugated secondary antibody for 90 min at room temperature. Protein bands were visualized by ECL luminescence reagent (Yeasen, China; Cat. No. 36222ES60) and captured with a chemiluminescence imager (Azure C280, USA); band intensities were quantified with ImageJ. A complete list of antibodies and dilutions is provided in Table S2.

Enzyme-linked immunosorbent assay analysis (ELISA)

Culture cells overnight and harvest the supernatant. Use TNF-α kit (Bio-Swamp, USA; Cat. No. HM10001) and LDH kit (Shanghai Enzyme Linked Biotechnology Co., Ltd., China; Cat. No. ml063227) to measure the absorbance (OD) at 450 nm with a FilterMax F3 fluorescence microplate reader.

Statistical analysis

Data analysis was performed using SPSS software. Normality and homogeneity of variance were verified using the Shapiro-Wilk and Levene's tests, respectively. Time-course data (CCK-8 and tumor growth) were analyzed by two-way repeated-measures ANOVA. Single-time-point multi-group comparisons used one-way ANOVA with Tukey's test. Outcomes were depicted as the mean ± standard deviation, with statistical significance denoted by $P<0.05$.

Results

The association between DPAGT1 and Siglec-15 expression levels in HCC and overall survival

DPAGT1 and Siglec-15 were significantly upregulated in HCC tissues compared with adjacent normal tissues (**Figure 1A**). The Pearson correlation between DPAGT1 and Siglec-15 expression was statistically significant although biologically weak ($r = 0.13$, $P = 0.015$, **Figure 1B**). Kaplan-Meier analysis revealed that elevated DPAGT1 expression was significantly associated with unfavorable overall survival in HCC ($P = 0.045$, **Figure 1C**, left). In contrast, Siglec-15 expression levels did not reach statistical significance for association with overall survival ($P = 0.68$, **Figure 1C**, right).

Effects of Siglec-15 modulation on the proliferation, migration, and invasion of HepG2 cells

To characterize the functional role of Siglec-15 in HCC, we established HepG2 cell models with Siglec-15 overexpression (OE-Siglec-15) or knockdown (sh-Siglec-15), alongside corresponding negative controls (OE-NC and sh-NC). Successful modulation of Siglec-15 was confirmed by elevated mRNA and protein levels in the OE-Siglec-15 group and significantly reduced expression in the sh-Siglec-15 group compared with their respective controls (**Figure 2A**, **2B**). Functional assays demonstrated that Siglec-15 overexpression significantly promoted HepG2 cell proliferation (**Figure 2C-E**), migration (**Figure 2F**, **2G**), and invasion (**Figure 2H**, **2I**), whereas silencing Siglec-15 exerted the opposite effects.

Correlation between DPAGT1 and Siglec-15 expression

To investigate the relationship between DPAGT1 and Siglec-15 in HCC, HepG2 cells were

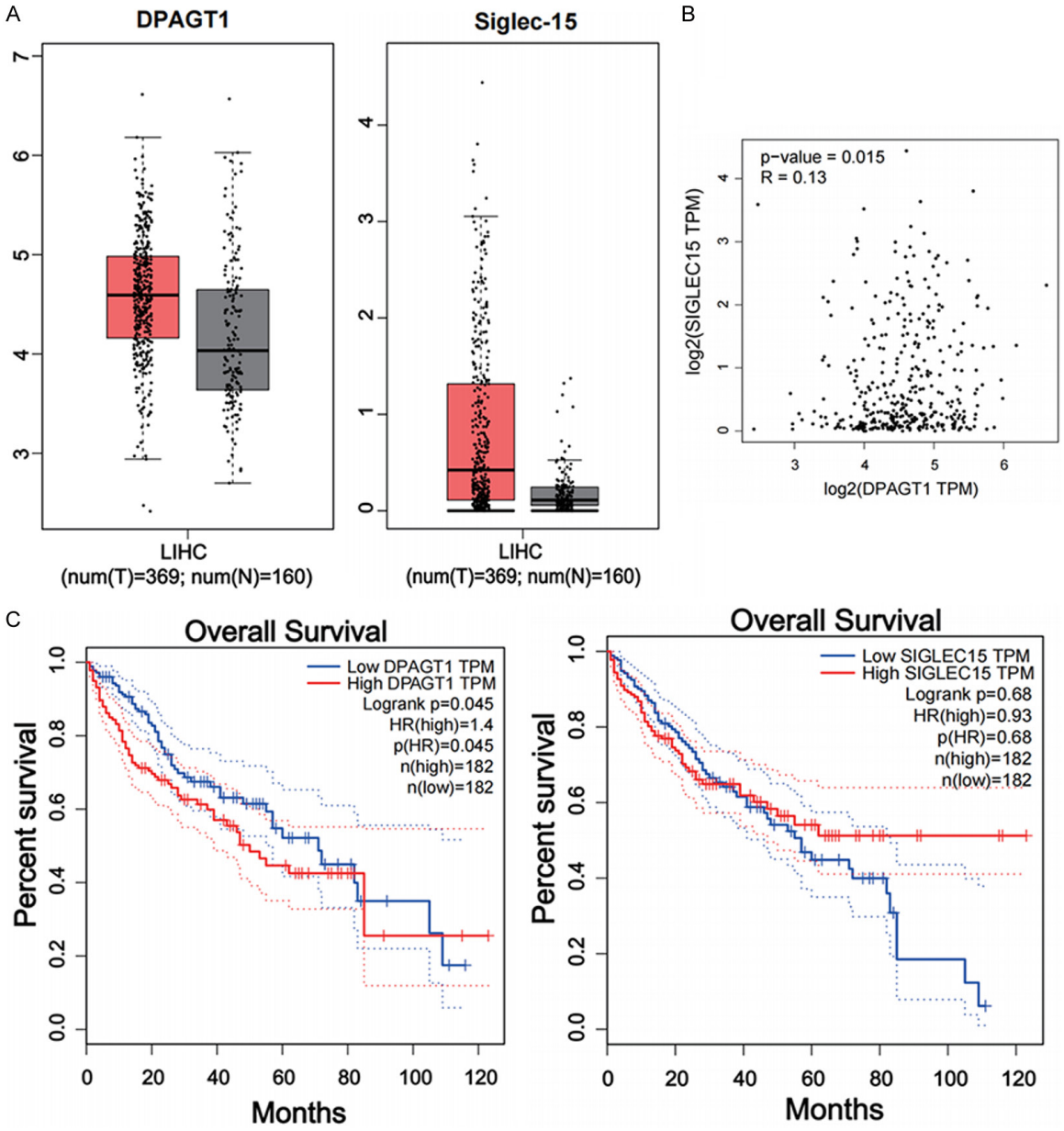

Figure 1. Expression profiles and prognostic significance of DPAGT1 and Siglec-15 in HCC. A. DPAGT1 and Siglec-15 expression levels in 369 tumor and 160 normal samples from the GEPIA database. B. Pearson correlation scatter plot of DPAGT1 and Siglec-15 expression. C. Kaplan-Meier curves for overall survival stratified by DPAGT1 (left) or Siglec-15 (right) expression. LIHC: liver hepatocellular carcinoma; N: normal; T: tumor; GEPIA: gene expression profiling interactive analysis.

transfected with DPAGT1 overexpression or knockdown constructs. DPAGT1 overexpression was associated with increased Siglec-15 mRNA and protein levels, whereas DPAGT1 knockdown led to reduced Siglec-15 expression (**Figure 3A-D**). Notably, ectopic overexpression of Siglec-15 did not fully rescue its protein expression levels in DPAGT1-silenced cells, suggesting that DPAGT1 may be involved in regulating Siglec-15 expression. Immunofluorescence staining further confirmed changes in Siglec-15 protein abundance following DPAGT1 modulation (**Figure 3E**). Co-immunoprecipitation analysis showed that Siglec-15 was detected in DPAGT1 immunoprecipitates (**Figure 3F**), suggesting that DPAGT1 and Siglec-15 may coexist in a shared biochemical complex.

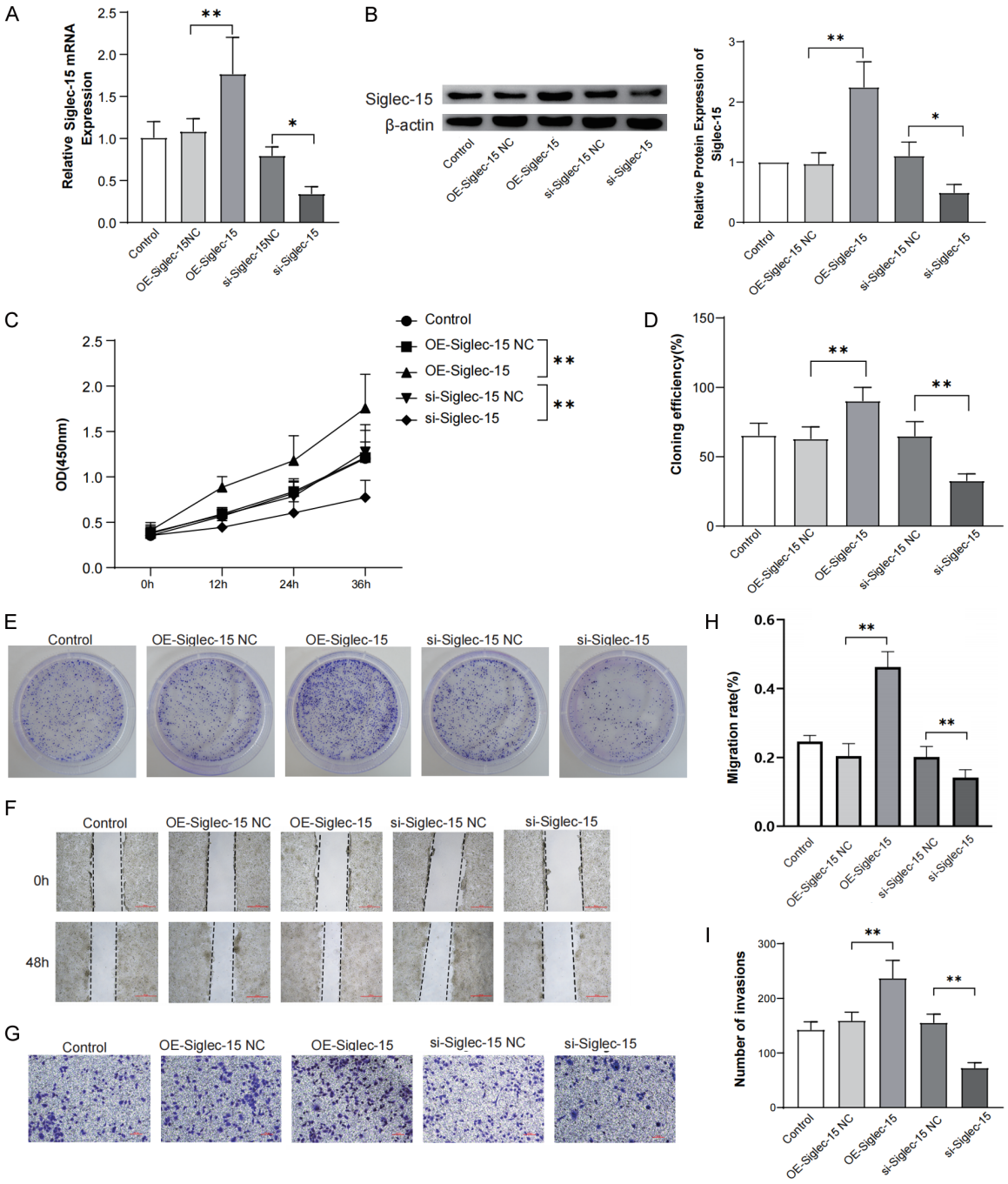

Figure 2. Effects of Siglec-15 modulation on HepG2 cell phenotype. (A, B) Siglec-15 mRNA (A) and protein (B) levels following overexpression or silencing. (C) CCK-8 assay results showing cell proliferation. (D, E) Colony formation assay result. (F, G) Wound healing assay results (Scale bar = 500 μm, 100×). (H, I) Transwell invasion assay results (Scale bar = 100 μm, 200×). Data were analyzed using one-way ANOVA or two-way repeated-measures ANOVA. **P*<0.05, ***P*<0.01.

Functional link between DPAGT1 and Siglec-15 in HepG2 cells

In HepG2 cells, overexpression of DPAGT1 correlated with enhanced proliferation, migration, and invasion, whereas knockdown of DPAGT1 suppressed these phenotypes. Notably, concurrent re-expression of Siglec-15 partially rescued the inhibitory phenotypes induced by DPAGT1 knockdown (**Figure 4**).

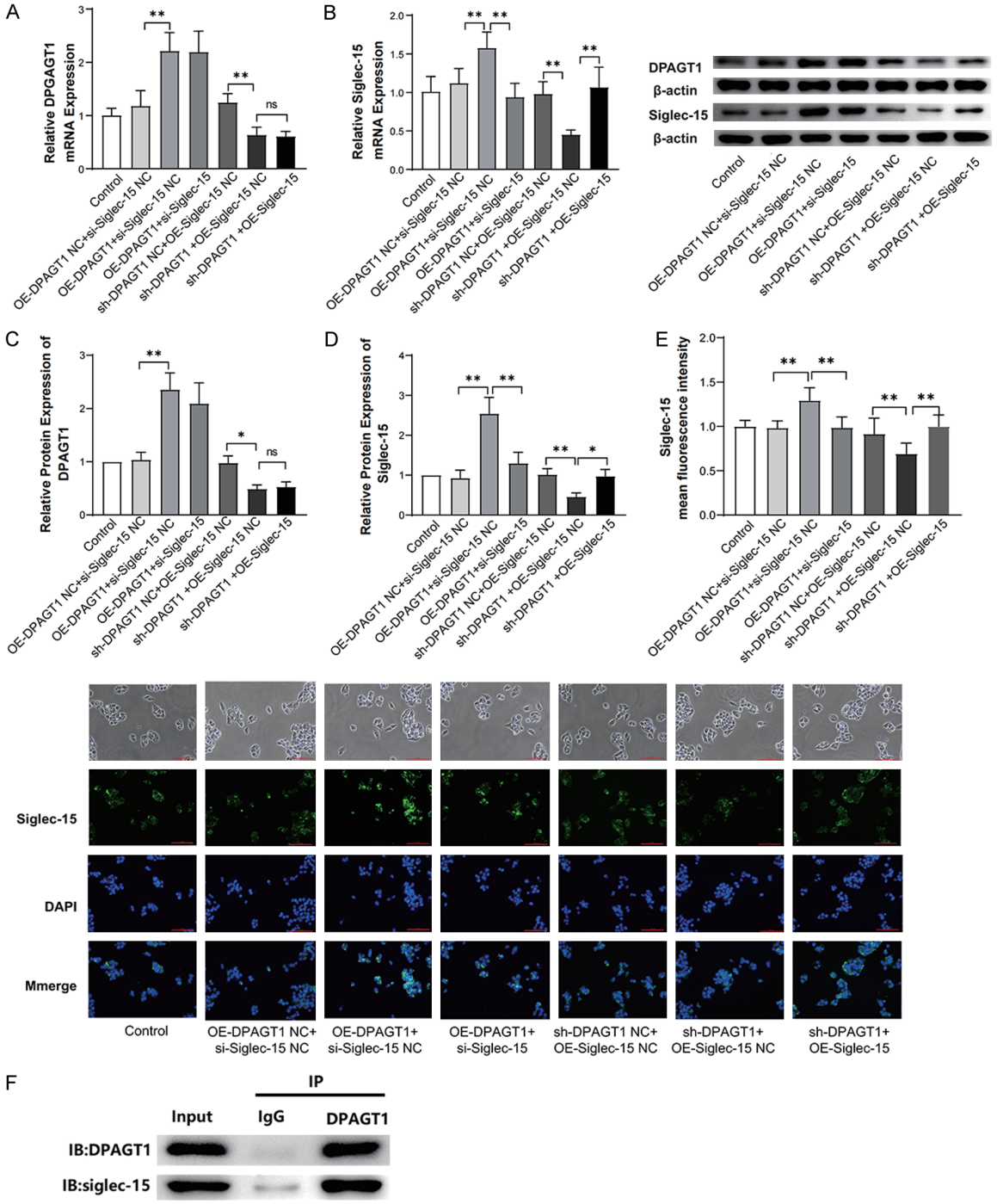

Figure 3. Modulation of DPAGT1 and Siglec-15 expression in HepG2 cells. (A, C) DPAGT1 mRNA (A) and protein (C) levels following DPAGT1 overexpression or knockdown. (B, D) Siglec-15 mRNA (B) and protein (D) levels following DPAGT1 or Siglec-15 modulation. (E) Immunofluorescence staining showing Siglec-15 protein expression under different transfection conditions (Scale bar = 100 μm, 200×). (F) Co-immunoprecipitation (Co-IP) analysis demonstrating that Siglec-15 was present in DPAGT1 immunoprecipitates. Data were analyzed using one-way ANOVA. **P*<0.05, ***P*<0.01.

The expression of DPAGT1-Siglec-15 is associated with cell phenotype

In DPAGT1-overexpressing cells, Siglec-15 expression was increased, accompanied by elevated levels of TGF-β1 and p-AKT, as well as upregulation of the mesenchymal marker N-cadherin and downregulation of the epithelial marker E-cadherin. In contrast, DPAGT1 knockdown resulted in decreased expression

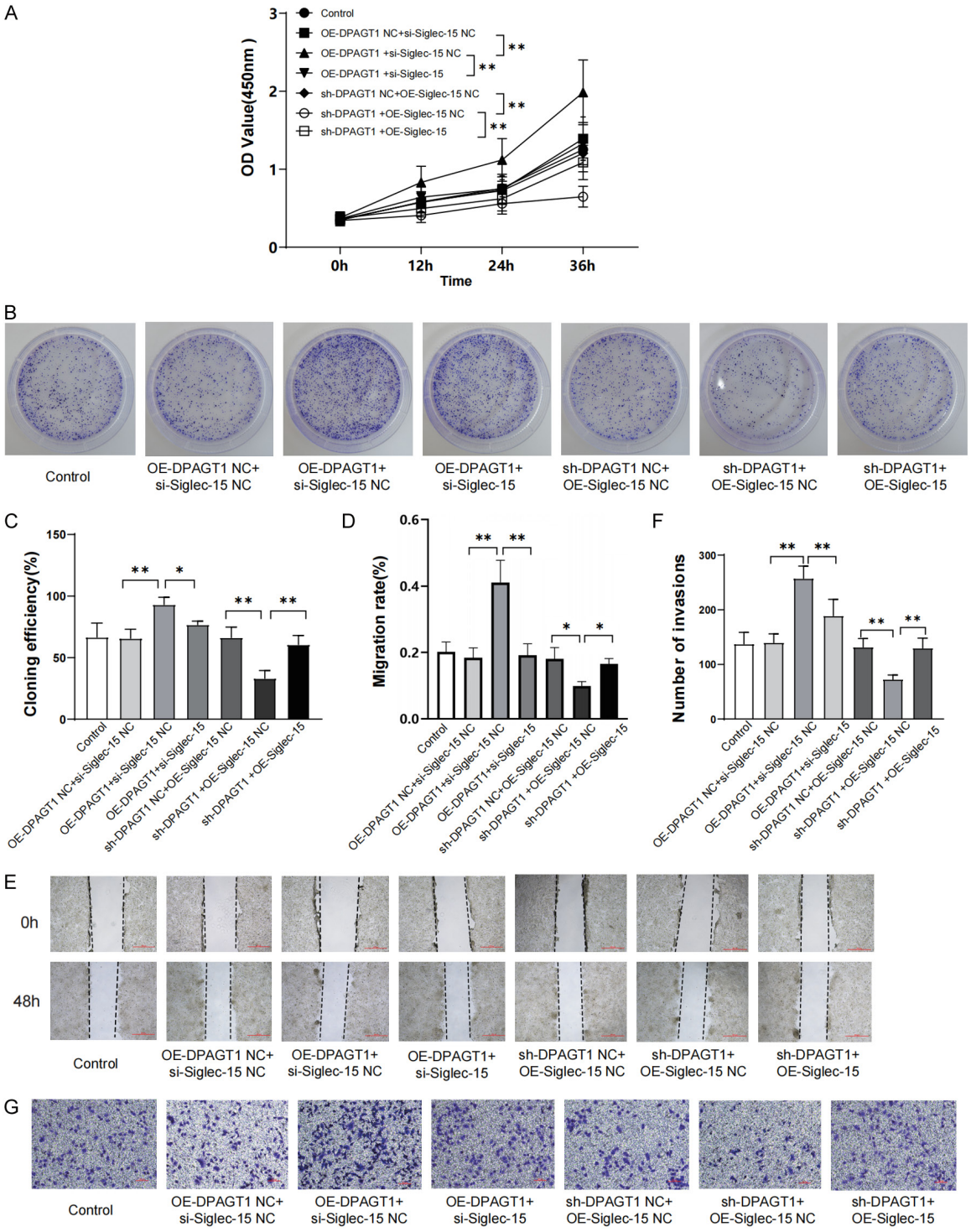

Figure 4. Functional interplay between DPAGT1 and Siglec-15 in HepG2 cells. A. CCK-8 assay results showing cell proliferation. B, C. Colony formation assay results. D, E. Wound healing assay results (Scale bar = 500 μm, 100×). F, G. Transwell invasion assay results (Scale bar = 100 μm, 200×). Data were analyzed using one-way ANOVA or two-way repeated-measures ANOVA. *P<0.05, **P<0.01.

of Siglec-15, TGF-β1, p-AKT, and N-cadherin, together with increased E-cadherin expression. Notably, re-expression of Siglec-15 in DPAGT1-knockdown cells partially restored these protein expression profiles (**Figure 5**).

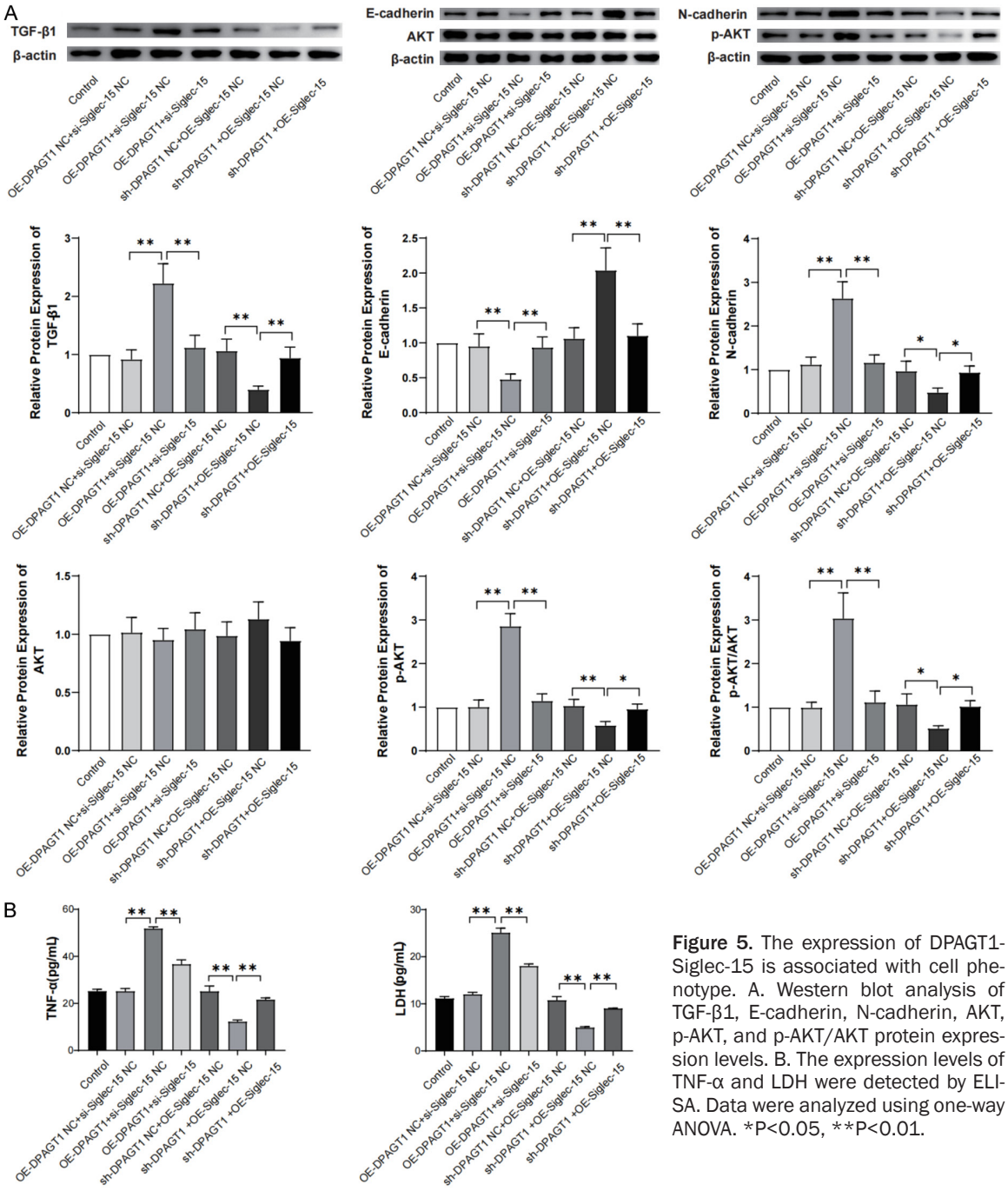

Figure 5. The expression of DPAGT1-Siglec-15 is associated with cell phenotype. A. Western blot analysis of TGF-β1, E-cadherin, N-cadherin, AKT, p-AKT, and p-AKT/AKT protein expression levels. B. The expression levels of TNF-α and LDH were detected by ELISA. Data were analyzed using one-way ANOVA. *P<0.05, **P<0.01.

Validation of DPAGT1-mediated phenotypes in Hep-3B cells

The effects of DPAGT1 modulation on cell phenotypes were further examined in a second HCC cell line, Hep-3B (**Figure 6**). Consistent with the findings in HepG2, DPAGT1 overexpression enhanced proliferation, migration, and invasion, whereas DPAGT1 knockdown suppressed these phenotypes. At the molecular level, DPAGT1 overexpression was associated with increased expression of Siglec-15, p-AKT, TGF-β1, N-cadherin, and Cyclin D1, as well as decreased E-cadherin expression.

In vivo role of DPAGT1 in Hep-3B xenografts

Hep-3B xenograft models demonstrated that DPAGT1 overexpression significantly promoted tumor growth, resulting in increased tumor vol-

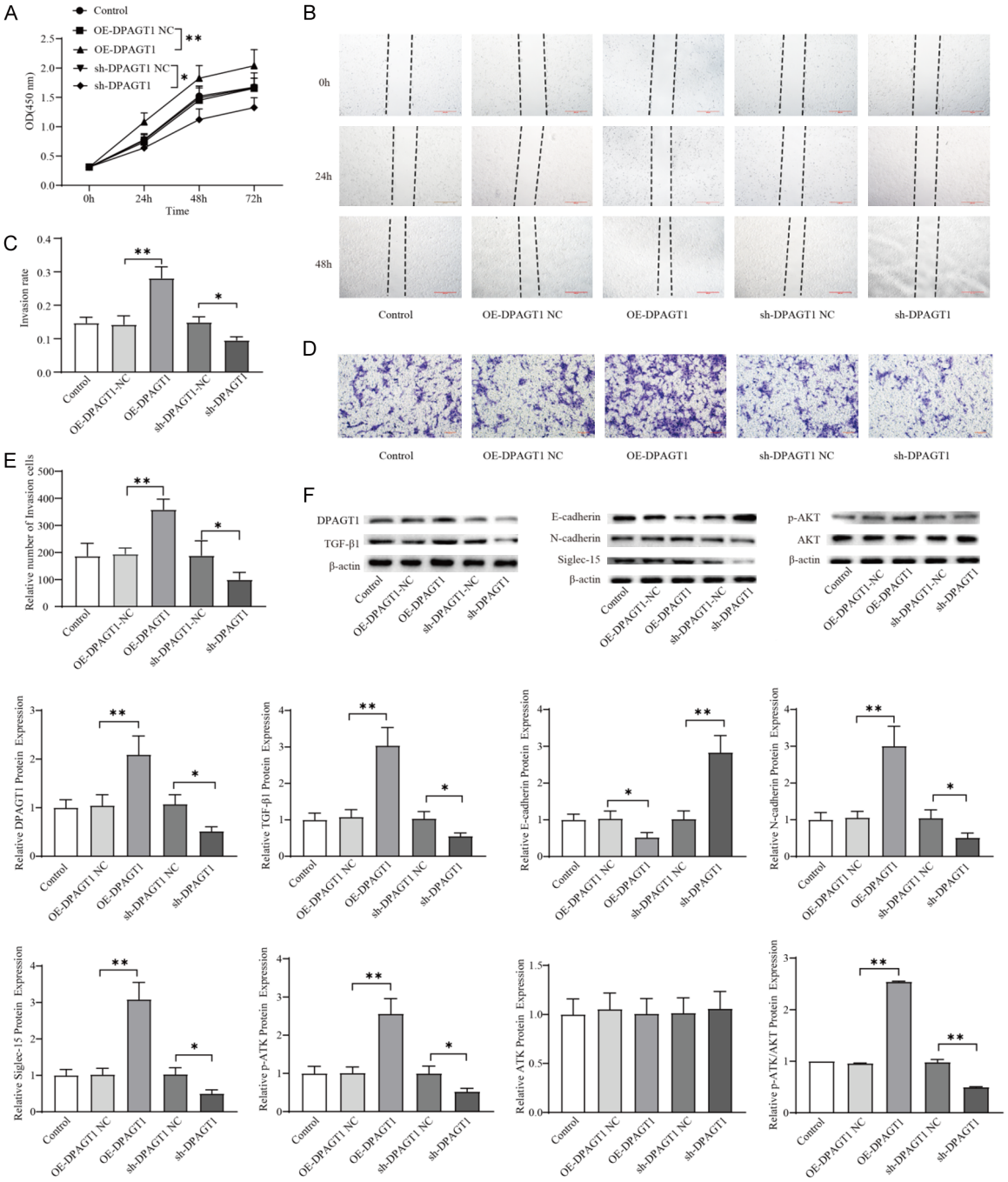

Figure 6. DPAGT1 promotes proliferation, migration, and invasion in Hep-3B cells. A. CCK-8 assay results showing cell proliferation. B, C. Wound healing assay results (Scale bar = 500 μm, 100×). D, E. Transwell invasion assay results (Scale bar = 100 μm, 200×). F. Western blot analysis; Data were analyzed using one-way ANOVA or two-way repeated-measures ANOVA. *P<0.05, **P<0.01.

ume and weight, whereas DPAGT1 knockdown markedly suppressed xenograft tumor progression (**Figure 7A-E**). Consistently, analysis of xenograft tissues showed that DPAGT1 overexpression upregulated Siglec-15, C-myc, N-cadherin, and Cyclin D1 expression while decreasing E-cadherin levels, whereas DPAGT1 depletion produced the opposite effects (**Figure 7F**, **7G**).

Discussion

HCC is a prevalent digestive system malignancy, ranking among the most common cancers

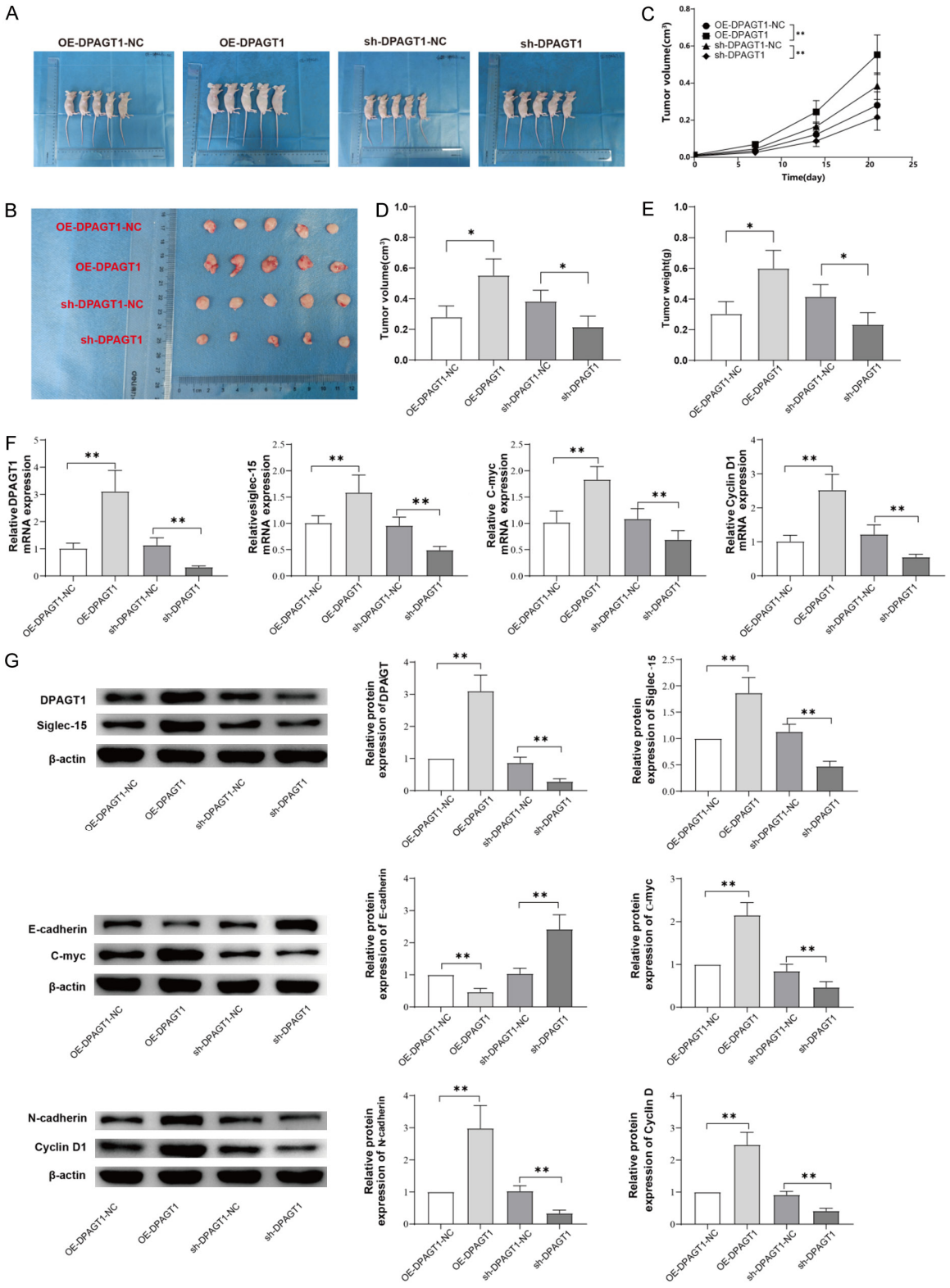

Figure 7. In vivo effects of DPAGT1 modulation in Hep-3B xenograft models. (A) Representative photographs of tumor-bearing mice from each group. (B) Representative photographs of excised tumors after euthanasia. (C) Tumor growth curves over the 21-day experimental period. (D) Terminal tumor volumes on day 21. (E) Terminal tumor weights. (F, G) Relative mRNA (F) and protein (G) expression levels of DPAGT1, Siglec-15, C-myc, Cyclin D1, N-cadherin, and E-cadherin (mean ± SD, n = 5). Data were analyzed using one-way ANOVA or two-way repeated-measures ANOVA. *P<0.05, **P<0.01.

worldwide. It stands as the sixth most common cancer in terms of incidence and the third in terms of mortality among all malignant neoplasms. Statistics reveal that HCC causes approximately 830,000 deaths annually [14]. Primary liver cancers are broadly categorized into three major types: HCC, cholangiocarcinoma, and hepatoblastoma, with HCC being the predominant type. In many countries, HCC constitutes over 90% of all primary liver cancers [15]. Although this disease can be treated using various approaches that can improve patient outcomes, the 5-year survival rate of patients with tumor recurrence, metastasis, and drug resistance remains disappointingly low (<5%) [16]. More effective treatment strategies are urgently needed to improve outcomes for patients with this devastating disease.

Glycosylation is the enzymatic modification of proteins and lipids by sugars. This process involves specific enzymes such as glycosidases and glycosyltransferases. Glycosylation is crucial for the addition of sugar groups to glycoproteins, endowing them with diverse functions [17]. Post-translational modifications, particularly glycosylation, critically regulate essential cellular processes, including proliferation, differentiation, and immune responses [18]. In cancer, glycosylation changes are often associated with enhanced tumor cell growth. These cells also exhibit increased invasion and metastasis. For example, glycans on cancer cells may promote proliferation by altering the cells' responses to growth factors. Shifts in glycosylation can also impact the function of immune cells within the tumor microenvironment. This can influence the tumor's capacity for immune evasion [19]. DPAGT1 is the first enzyme in the glycosyltransferase pathway. It plays a key role in the biosynthesis of N-glycans. Thus, modulation of DPAGT1 expression can regulate this biosynthesis [20].

Previous studies have indicated that DPAGT1 activity is associated with tumor cell invasion and disruption of intercellular adhesion [21, 22]. A reduction in DPAGT1 expression can decrease E-cadherin glycosylation and limit the Wnt signaling pathway [23]. DPAGT1 inhibitors have been shown to suppress tumor cell migration in various solid tumors. These DPAGT1 inhibitors include 2-deoxyglucose and analogs of tunicamycin and capuramycin [24, 25]. High DPAGT1 levels have been linked to the shedding of HER2-targeted proteins, which can lead to trastuzumab resistance and are associated with poor clinical outcomes [22]. In a mouse model of liver cancer, DPAGT1 was shown to enhance ABCG2 activity through activation of the hexosamine pathway. This mechanism may contribute to chemotherapy resistance [13]. In the present study, DPAGT1 expression was significantly elevated in HCC tissues compared with adjacent non-tumorous tissues. The tumor-promoting effects of DPAGT1 were consistently observed across two distinct HCC cell lines. DPAGT1 overexpression promoted cell proliferation, migration, and invasion in both HepG2 and Hep-3B cells, while DPAGT1 suppression counteracted these effects. These in vitro findings were further supported by in vivo experiments using Hep-3B xenograft models, in which DPAGT1 overexpression accelerated tumor growth, whereas DPAGT1 knockdown suppressed tumorigenesis. Moreover, DPAGT1 overexpression was accompanied by increased expression of Siglec-15, c-Myc, N-cadherin, and Cyclin D1, as well as decreased E-cadherin expression. However, the molecular mechanisms underlying the regulatory effects of DPAGT1 in HCC remain unclear.

Although anti-PD-1/PD-L1 therapies have achieved remarkable clinical success as a major class of cancer immunotherapies, a substantial proportion of patients fail to respond to these treatments [26]. Consequently, considerable efforts have been devoted to identifying alternative immune checkpoint targets, such as Siglec-15 [6, 27]. Although Siglec-15 is recognized as a potential immune suppressive molecule that inhibits T-cell activity within the tumor microenvironment [28, 29], its tumor cell-intrinsic functions remain poorly understood. Bioinformatic analysis of GEPIA data revealed Siglec-15 upregulation in HCC tissues, with a weak positive correlation to DPAGT1 expression ($r = 0.13$, $P<0.05$). Functional validation in HepG2 cells demonstrated that DPAGT1 overexpression or knockdown altered Siglec-15 expression, whereas manipulation of Siglec-15 expression did not affect DPAGT1 expression. These findings suggest that DPAGT1 and Siglec-15 coexist in a shared biochemical complex. Nevertheless, whether this reflects direct protein-protein interaction or indirect association mediated by glycosyl-

ation or ER-resident chaperones warrants further investigation.

The invasive capacity of cancer cells is closely associated with epithelial-mesenchymal transition (EMT), a cellular program characterized by changes in cell adhesion and motility. E-cadherin and N-cadherin are key molecular markers involved in EMT regulation [30, 31]. Consistent with previous reports, DPAGT1 silencing in HepG2 cells was associated with increased E-cadherin expression and decreased N-cadherin expression. Notably, concurrent Siglec-15 overexpression partially rescued these EMT marker alterations induced by DPAGT1 knockdown. This suggests that Siglec-15 may contribute to the phenotypic changes induced by DPAGT1 modulation. Furthermore, the alterations in TGF-β1 and p-AKT induced by DPAGT1 knockdown were partially reversed by subsequent Siglec-15 re-expression. Collectively, these findings suggest that DPAGT1 and Siglec-15 may participate in the regulation of EMT-related processes and malignant phenotypes in HCC cells.

Limitations

While this study provides evidence supporting a functional association between DPAGT1 and Siglec-15, several limitations should be acknowledged. First, the functional rescue of DPAGT1 knockdown by Siglec-15 re-expression was demonstrated only in HepG2 cells. Although DPAGT1-mediated phenotypes were consistently observed in both HepG2 and Hep-3B cells, the DPAGT1-Siglec-15 functional interaction remains to be validated in additional HCC cell lines, including Hep-3B. Second, the precise molecular mechanism underlying the DPAGT1-Siglec-15 relationship remains unresolved. Current evidence is insufficient to determine whether their association reflects direct physical interaction or an indirect regulatory effect mediated by glycosylation processes or ER-resident chaperones. Future studies will extend validation to additional HCC models and clarify the underlying biochemical mechanisms.

Conclusions

This study demonstrates that DPAGT1 contributes to HCC progression and is functionally associated with Siglec-15. DPAGT1 overexpression promoted proliferation, migration, and EMT-related phenotypes, whereas DPAGT1 knockdown suppressed these malignant behaviors. Re-expression of Siglec-15 partially rescued the inhibitory effects induced by DPAGT1 knockdown. Collectively, these findings identify DPAGT1 as a promoter of HCC progression and suggest a potential functional interplay between DPAGT1 and Siglec-15 in regulating EMT-related phenotypes.

Acknowledgements

This research was funded by the Guangxi Key Technologies R&D Program (No. Guike AB24010163).

Disclosure of conflict of interest

None.

Address correspondence to: Min Luo, Department of Oncology, The Second Nanning People's Hospital, No. 13 Dancun Road, Jiangnan District, Nanning 530021, Guangxi, China. Tel: +86-0771-4808089; E-mail: 13347606605@163.com

References

[1] Ganesan P and Kulik LM. Hepatocellular carcinoma: new developments. Clin Liver Dis 2023; 27: 85-102.
[2] Brown ZJ, Tsilimigras DI, Ruff SM, Mohseni A, Kamel IR, Cloyd JM and Pawlik TM. Management of hepatocellular carcinoma: a review. JAMA Surg 2023; 158: 410-20.
[3] Singh SP, Madke T and Chand P. Global epidemiology of hepatocellular carcinoma. J Clin Exp Hepatol 2025; 15: 102446.
[4] Toh MR, Wong EYT, Wong SH, Ng AWT, Loo LH, Chow PK and Ngeow J. Global epidemiology and genetics of hepatocellular carcinoma. Gastroenterology 2023; 164: 766-82.
[5] Kirsh J, Kaudeer YB, Li YE and Clemons B. BPS2026–DPAGT1: anticancer target and model phosphoglycosyltransferase. Biophys J 2026; 125: 345a.
[6] Li L, Wang L, Liu Q, Ye Y, Lei Q, Li C, Guo X, Nian S and Yuan Q. The role of Siglec-15 in tumor immunity: mechanisms and therapy. Mol Cancer Ther 2026; 25: 717-26.
[7] Shafi S, Aung TN, Xirou V, Gavrielatou N, Vathiotis IA, Fernandez A, Moutafi M, Yaghoobi V, Herbst RS, Liu LN, Langermann S and Rimm DL. Quantitative assessment of Siglec-15 expression in lung, breast, head, and neck squamous cell carcinoma and bladder cancer. Lab Invest 2022; 102: 1143-1149.
[8] Kurosu M and Mitachi K. DPAGT1-perspective as an anticancer drug target. Molecules 2025; 30: 4049.

[9] He M, Zhou X and Wang X. Glycosylation: mechanisms, biological functions and clinical implications. Signal Transduct Target Ther 2024; 9: 194.
[10] Khorami-Sarvestani S, Hanash SM, Fahrmann JF, León-Letelier RA and Katayama H. Glycosylation in cancer as a source of biomarkers. Expert Rev Proteomics 2024; 21: 345-65.
[11] Zheng L, Yang Q, Li F, Zhu M, Yang H, Tan T, Wu B, Liu M, Xu C, Yin J and Cao C. The glycosylation of immune checkpoints and their applications in oncology. Pharmaceuticals (Basel) 2022; 15: 1451.
[12] Fu B, Chen J, Liu X, Li J, Feng X, Wang J, Li Y, Zhang Y, Ma J, Wang Y, Gu B, Zhang Y and Lu H. Large-scale serum N-glycomics tracks N-glycosylation dynamics in hepatocellular carcinoma progression and enables early diagnosis. Nat Commun 2026; 17: 1885
[13] Li R, Xu T, Wang H, Wu N, Liu F, Jia X, Mi J, Lv J and Gao H. Dysregulation of the miR-325-3p/DPAGT1 axis supports HBV-positive HCC chemoresistance. Biochem Biophys Res Commun 2019; 519: 358-365.
[14] Singal AG, Kanwal F and Llovet JM. Global trends in hepatocellular carcinoma epidemiology: implications for screening, prevention and therapy. Nat Rev Clin Oncol 2023; 20: 864-84.
[15] Cho Y, Kim BH and Park JW. Overview of Asian clinical practice guidelines for the management of hepatocellular carcinoma: an Asian perspective comparison. Clin Mol Hepatol 2023; 29: 252-262.
[16] Calderon-Martinez E, Landazuri-Navas S, Vilchez E, Cantu-Hernandez R, Mosquera-Moscoso J, Encalada S, Al Lami Z, Zevallos-Delgado C and Cinicola J. Prognostic scores and survival rates by etiology of hepatocellular carcinoma: a review. J Clin Med Res 2023; 15: 200-207.
[17] Xu X, Peng Q, Jiang X, Tan S, Yang W, Han Y, Oyang L, Lin J, Shen M, Wang J, Li H, Xia L, Peng M, Wu N, Tang Y, Wang H, Liao Q and Zhou Y. Altered glycosylation in cancer: molecular functions and therapeutic potential. Cancer Commun (Lond) 2024; 44: 1316-36.
[18] Bangarh R, Khatana C, Kaur S, Sharma A, Kaushal A, Siwal SS, Tuli HS, Dhama K, Thakur VK, Saini RV and Saini AK. Aberrant protein glycosylation: implications on diagnosis and immunotherapy. Biotechnol Adv 2023; 66: 108149.
[19] Lin Y and Lubman DM. The role of N-glycosylation in cancer. Acta Pharm Sin B 2024; 14: 1098-110.
[20] Cheng Q, Hu X, Zhang X, Yang D, Zhao G, Sun L, Jiang M, Yang L, Cai J, Wang B, Zhang M, Han F, Li Y and Nie H. N-glycosylation at N57/100/110 affects CD44s localization, function and stability in hepatocellular carcinoma. Eur J Cell Biol 2023; 102: 151360.
[21] Di Gregorio J, Di Giuseppe L, Terreri S, Rossi M, Battafarano G, Pagliarosi O, Flati V and Del Fattore A. Protein stability regulation in osteosarcoma: the ubiquitin-like modifications and glycosylation as mediators of tumor growth and as targets for therapy. Cells 2024; 13: 537.
[22] Yang M, Li Y, Kong L, Huang S, He L, Liu P, Mo S, Lu X, Lin X, Xiao Y, Shi D, Huang X, Chen B, Chen X, Ouyang Y, Li J, Lin C and Song L. Inhibition of DPAGT1 suppresses HER2 shedding and trastuzumab resistance in human breast cancer. J Clin Invest 2023; 133: e164428.
[23] Sengupta PK, Bouchie MP, Nita-Lazar M, Yang HY and Kukuruzinska MA. Coordinate regulation of N-glycosylation gene DPAGT1, canonical Wnt signaling and E-cadherin adhesion. J Cell Sci 2013; 126: 484-496.
[24] Mitachi K, Kansal RG, Hevener KE, Gillman CD, Hussain SM, Yun HG, Miranda-Carboni GA, Glazer ES, Clemons WM Jr and Kurosu M. DPAGT1 inhibitors of capuramycin analogues and their antimigratory activities of solid tumors. J Med Chem 2020; 63: 10855-10878.
[25] Ibezim A, Osigwe S, Uzor P, Engel N, Ramanathan K and Nwodo N. Computational studies reveal potential dolichyl-phosphate N-acetylglucosaminephosphotransferase inhibitors amidst existing drugs. J Biomol Struct Dyn 2023; 41: 4811-4818.
[26] Zhang H, Liu L, Liu J, Dang P, Hu S, Yuan W, Sun Z, Liu Y and Wang C. Roles of tumor-associated macrophages in anti-PD-1/PD-L1 immunotherapy for solid cancers. Mol Cancer 2023; 22: 58.
[27] Liu Q, Li L, Nian S, Sun X, Guo X, Li C, Yang Z, Ye Y and Yuan Q. Development of a novel anti-Siglec-15 antibody for tumor immunotherapy. Immunotargets Ther 2025; 14: 1419-35.
[28] Jiang KY, Qi LL, Liu XB, Wang Y and Wang L. Prognostic value of Siglec-15 expression in patients with solid tumors: a meta-analysis. Front Oncol 2023; 12: 1073932.
[29] Sun J, Lu Q, Sanmamed MF and Wang J. Siglec-15 as an emerging target for next-generation cancer immunotherapy. Clin Cancer Res 2021; 27: 680-688.
[30] Celià-Terrassa T and Kang Y. How important is EMT for cancer metastasis? PLoS Biol 2024; 22: e3002487.
[31] Manfioletti G and Fedele M. Epithelial-mesenchymal transition (EMT). Int J Mol Sci 2023; 24: 11386.

Table S1. Primer sequence

Primer		Sequence (5'-3')
DPAGT1	F	GCATATCATCCCCTGCCCTC
DPAGT1	R	GTGCCCAAGAAAGAGAGGCT
SIGLEC	F	CTGTGGTCCTTGGGGCTTAG
SIGLEC	R	GGCCTCGTTATTCCCCTAGC
C-MYC	F	CCTACCCTCTCAACGACAGC
C-MYC	R	TCTTGACATTCTCCTCGGTG
CYCLIN D1	F	TGCACCACCAACTGCTTAGC
CYCLIN D1	R	GGATGGAGTTGTGCAGATGT
ACTB	F	CGTAAAGACCTCTATGCCAACA
ACTB	R	TCCTTCTGCATCCTGTCAGC

Table S2. Information of antibodies used in Western blot assay

Antibodies	Catalog	Dilution rate	Manufacturer
β-Actin	3700S	1:2000	Cell signaling technology
E-cadherin	20874-1-AP	1:2000	Proteintech
N-cadherin	ab76011	1:2000	Abcam
DPAGT1	ab99518	1:2000	Abcam
Siglec-15	ab205921	1:2000	Abcam
AKT	4691	1:2000	Cell signaling technology
p-AKT	9271	1:2000	Cell signaling technology
TGF-β1	ab215715	1:2000	Abcam
C-myc	ab32072	1:1000	Abcam
Cyclin D1	ab16663	1:500	Abcam
Goat Anti-Rabbit IgG	ab205718	1:8000	Abcam
Goat Anti-Mouse IgG	ab205719	1:8000	Abcam